Energy 248 (2022) 123593

Contents lists available at ScienceDirect

Energy

journal homepage: www.elsevier.com/locate/energy

Fuel injection strategy optimisation and experimental performance and emissions evaluation of diesel displacement by port fuel injected methanol in a retrofitted mid-size genset engine prototype

Avinash Kumar Agarwal*, Vikram Kumar, Ashutosh Jena, Ankur Kalwar

Engine Research Laboratory, Department of Mechanical Engineering, Indian Institute of Technology Kanpur, Kanpur, 208016, India

ARTICLE INFO

Article history:
Received 27 September 2021
Received in revised form
26 January 2022
Accepted 24 February 2022
Available online 25 February 2022

Keywords:
Methanol
Combustion
Emissions
Genset
Dual-fuel engine

ABSTRACT

The reliance of the transport, agriculture, marine, and power generation sectors on heavy-duty diesel engines would continue in the foreseeable future due to their higher efficiency, torque, fuel economy, and durability, despite growing concerns about emissions. This dependence would rise further due to the unavailability of an equally efficient alternative prime mover having a similar or better power density. The adoption of alternative fuels has emerged as a promising solution to tackle emission issues. Methanol has exhibited great potential to reduce pollutants by adopting advanced combustion technologies among various new fuels. Retrofitment of existing engines can be a viable solution for methanol adaptation because engine design modifications are not practical for on-field engines. The present study focused on evaluating the performance and emissions of a commercial Genset CI engine adapted to operate using diesel-methanol dual-fuel combustion (DFC) technology, which required very few hardware modifications to facilitate retrofitment for methanol adaptation. Inlet charge temperature was controlled using hot air from the turbocharger. Port fuel injection was used to induct methanol into the engine manifold, and a premixed charge entered the engine combustion chamber. This charge was ignited by spraying diesel directly into the engine combustion chamber. The engine's performance and emissions were compared with the OEM configuration (diesel fuelling mode) at methanol's low, medium, and high diesel replacement. The fuel injection parameters (injection timing and pressure) of diesel were varied to obtain optimum fuel injection strategies for various engine loads. A sharp increase in thermal efficiency was observed at 30% diesel displacement (on an energy basis) by methanol at a 9 kW generator load. In contrast, a slight penalty in thermal efficiency was observed at 80% diesel displacement (on an energy basis) by methanol. Higher HC and CO emissions were also observed for the engine using higher methanol fractions. The CO_2 emission was comparable to or less than the OEM diesel configuration at identical loads. Exhaust smoke was considerably lower for methanol-fuelled operation, indicating a significant reduction in particulates in the engine exhaust. Advancing fuel injection timings and higher fuel injection pressure of diesel proved to be a good strategy for methanol adaptation in genset engines, with an acceptable cylinder noise.

1. Introduction

Methanol has emerged as a promising low-carbon fuel for internal combustion (IC) engines. Methanol can be easily synthesised from various feedstocks, such as municipal solid waste (MSW), high ash coals, low-value biomass waste etc. [1,2]. Its production scalability is one of the prime reasons for methanol garnering serious attention and investment as a long-term sustainable fuel for the transport sector. It can be produced by thermochemical processes (e.g., biomass gasification) instead of biological processes, which significantly increases its energetic yield and avoids conflict with the global food supply chain. Combined ethanol/methanol production plants have been proposed to have higher energetic yields, along with a lower carbon footprint [3]. Interestingly, liquid methanol has 40% more hydrogen per unit storage volume than liquid hydrogen (LH_2), which suffers from severe energy requirements essential for liquefication and storage [4]. Methanol

* Corresponding author.
E-mail address: akag@iitk.ac.in (A.K. Agarwal).

https://doi.org/10.1016/j.energy.2022.123593
0360-5442/

production from atmospheric CO_2 is an open area for research for limitless methanol production and sustainable methanol and global economy [5–7].

Methanol draws criticism for its toxicity; however, a large-scale vehicle trial of M85 in California reported zero cases due to its toxicity. Higher octane rating makes it an excellent alternative to gasoline for simultaneously enhancing the engine power density and reducing emissions. However, low cetane number and lower viscosity and lubricity make it an inferior candidate for diesel replacement in compression ignition (CI) engines. Despite these challenges, enormous research efforts are being directed to adopt methanol in CI engines. The low reactivity of methanol makes its auto-ignition difficult in the compression ignition mode in a diesel cycle. The low viscosity and inherent lack of lubricity of methanol create lubrication issues in conventional diesel injection systems such as high-pressure pumps and fuel injectors. Several lubricity additives have been used in previous studies to improve the lubricity of methanol [8]. Cetane improvers have also been attempted to utilise 100% methanol via a high-pressure direct injection system in CI engines [9,10]. Pilot diesel injection is another possibility to assist the ignition of methanol by increasing the in-cylinder temperature. Several possibilities have been explored for this approach. Dong et al. used two separate HPDI injectors for methanol and diesel [11]. However, it remains a complex design challenge to accommodate two injectors in the crowded cylinder head. However, this approach can provide a practical solution for large bore engines with uncongested cylinder heads and research to further develop this technology. Wartsila developed a more practical solution for methanol adaptation in a DFC mode CI engine [12]. A coaxial injector was developed for methanol and diesel injection from a single injector. However, this technology is still in its infancy and is largely applicable to large-bore engines, with little practical importance for smaller engines. Methanol fumigation/port injection is another common and more straightforward approach for methanol adaptation via DFC in diesel engines [12,13]. This technology is similar to diesel/CNG dual-fuel technology, which is well-proven for CNG buses. Methanol-diesel DFC engines are also under development and are not commercialised yet. Several researchers have investigated the performance and emissions of the prototype engines developed using various methanol adaptation strategies. Verhelst et al. [14] extensively reviewed methanol utilisation approaches in the engine. The primary objective of this review was to investigate the impact of methanol on the NOx-PM trade-off.

Ma et al. suggested that premixed methanol-air charge was the main energy source and pilot diesel reduced the soot emissions from the engine using this approach [15]. A higher latent heat of vaporisation of methanol reduced the peak combustion temperature, resulting in lower NOx formation in the engine [16–18]. Panda et al. [19] investigated methanol DFC mode operation using different diesel injection strategies in a constant speed engine. They reported that the pilot-main strategy yielded higher brake-specific NOx (BSNOx) emissions due to rapid combustion. Soot emissions also reduced due to shorter ignition delays. They concluded that a pilot-main-post injection strategy for diesel could be the most appropriate one for an overall reduction in emissions. Liu et al. [18] investigated the effect of fuel injection pressure (FIP) on the heavy-duty engine performance and emissions in DFC mode. Increased FIP resulted in higher NOx emissions, lower soot emissions, and improved brake-specific fuel consumption (BSFC). Krishnamurthy et al. [20] compared the emissions of gasoline/toluene with methanol in a DFC mode constant speed stationary engine. They reported significantly lower NOx emissions from methanol compared to baseline gasoline. The lowest soot emissions were exhibited by methanol-diesel DFC mode operation. This study suggested methanol as the best alternative to be used as a primary fuel in DFC mode CI engines. Other than these, most studies focused on developing fuel injection strategies in engines operating at constant load and speed. Some studies reported over 50% reduction in NOx emissions across the engine operating range.

Several studies focused on methanol substitution fraction in DFC mode. Optimising methanol fraction in DFC mode engines remains one of the main challenges. The maximum power with methanol substitution is limited by knocking in rich mixtures. On the other hand, the lean limit makes it susceptible to unstable combustion and misfire, leading to higher unburn hydrocarbon (UHC) emissions. Guan et al. [21] reported that a maximum of 28% diesel displacement by methanol was possible in a heavy-duty diesel engine with an acceptable rate of pressure rise (RoPR). Saxena et al. [22] reported that combustion instability increased with increasing methanol fuel energy percentage, i.e., premixed ratio. However, lower peak in-cylinder pressure (P_{max}) increased with increasing MPR at all loads. The authors reported higher UHC and CO emissions and increased nucleation mode particles (NMP) from methanol fuelling mode than baseline diesel mode. Dou et al. [23] investigated the effect of pilot diesel's premixed ratio and injection timing on the emission characteristics of the engine. They reported that retarded injection timing is beneficial at a higher premixed ratio for mitigating particulate emissions. A maximum of 85% diesel displacement has been reported in the literature, but the maximum diesel displacement by methanol depends on engine design, boost, and valve timings [12,24].

Methanol DFC mode engine operation exhibits increased UHC and CO emissions since the premixed methanol-air mixture easily enters the crevices and squish regions in a DFC engine. Therefore, modified piston designs with reduced squish area exhibit a reduction in UHC emissions. Researchers have also explored multiple diesel pilot injection strategies. Advanced pilot injection increased the charge reactivity in the squish region, promoting the completion of combustion. Several researchers have reported lower HC emissions from this approach [25]. Evaporative cooling of methanol resulted in lower charge temperature, which reduced the peak in-cylinder temperature during combustion. Lower in-cylinder temperature was responsible for less intense ambient conditions for oxidation of hydrocarbons, thereby increasing HC emissions. Pan et al. [26] investigated air preheating to address this issue, and a successful reduction in HC emissions was achieved; however, this approach led to increased NOx emissions.

From the previous research studies summarised above, it can be concluded that methanol can be adopted in CI engines with few hardware modifications. Still, it leads to some penalties in HC and CO emissions. However, these hardware modifications are required to be kept to a minimum for the retrofitment of existing diesel engines for faster adaption of methanol in the transport sector. Therefore, a detailed study should be carried out in a commercial diesel engine with minimum possible hardware modifications for methanol adaptation in an existing diesel engine. A two-cylinder Genset engine has been adapted for methanol by suitable hardware modifications in this study to explore this further. The test engine is popularly used in Gensets for power backup in offices, commercial establishments, industries, and residential apartments. The test engine was modified for DFC mode operation using methanol and diesel, and the ECU was recalibrated/optimised for duel-fuel operation. Detailed engine performance and emissions investigations were conducted, and then the results were compared with the unmodified engine with OEM ECU calibration using diesel-only fuelling.

2. Experimental setup and methodology

A two-cylinder, four-stroke, turbocharged-intercooled, common

rail direct injection (CRDI) Genset engine (FG Wilson Diesel Generator) was used for conducting the experiments. The technical specifications of the test engine are given in Table 1, and the schematic of the experimental setup is shown in Fig. 1. A resistive load bank was used for loading the alternator, which in turn loaded the engine. Few hardware modifications were done in the test engine for operating it in methanol-diesel DFC mode.

The OEM electronic control unit (ECU) was replaced with an open ECU (Motec; M142 GPR Diesel). The open ECU was used to modify the diesel injection parameters such as fuel injection timing, FIP, and injected fuel mass per cycle with greater flexibility. The injected fuel mass for diesel was changed by changing the ECU map's cell value (fuel mass in mg) (Throttle vs RPM). Therefore, for changing the FIP, the injector's pulse width (pulse width map: FIP vs fuel mass) changed to meet the cell value according to the injector calibration curve. An inlet meter valve mounted on a high-pressure pump was controlled via ECU, which controlled the diesel flow rate to maintain the desired rail and diesel injection pressures. The diesel injection timing was controlled by actuating the injector based on the timings set in the ECU timing map. On the other hand, the methanol injection system was not linked with the open ECU. Its injection quantity was controlled via another Arduino-based fuel injection system, in which methanol port fuel injection was controlled by the pulse width (injection duration) modulation. Methanol injection in the inlet manifold was achieved by installing a port fuel injection (PFI) system. Methanol was injected during the intake stroke in the engine cycle using a separate fuel injector and a feed pump. Methanol injection quantity was controlled by a customised microcontroller-based (Arduino) system in each engine cycle. The methanol injector was mounted in an intake manifold plenum, which is cubical, having considerable volume for spray-air mixing with lesser chances of fuel impingement. Downstream of the plenum, two separate intake ports for both cylinders were located. The multi-hole PFI injectors used in this study had a spray penetration length of ~80 mm at 3.5 bar injection pressure [27], which was as per the dimensions of the plenum.

A higher enthalpy of vaporisation of methanol reduces the intake charge temperature considerably in a high methanol substitution ratio. In addition, the engine's inlet air system was modified to maintain the incoming air temperature constant by partially (or completely) bypassing the intercooler located downstream of the turbocharger. Air from the intercooler and the hot bypass were mixed in the inlet manifold. Their respective valves adjusted the hot and cold air proportions to achieve the desired steady-state inlet air temperature. The methanol injector was placed downstream of the turbocharger and intercooler. A single-point methanol injection system was employed in the intake plenum (cubical), after which intake ports for both the cylinders were located.

The fuel consumption rate of diesel and methanol were measured using the burette fuel measurement method. Inlet air flow rate measurement was done using a laminar flow element (LFE). Regulated exhaust emissions (HC, CO, NOx, and CO_2) were measured using a Horiba emission gas analyser (Horiba; MEXA-584L), and the smoke opacity was measured using a smoke opacimeter (AVL; 437).

The engine tests were performed at a fixed speed of 1500 rpm at four Generator loads (20, 40, 60, and 80% corresponding to 3, 6, 9, and 12 kW, respectively). The expression used to obtain methanol premixed ratio (MPR) is:

$$MPR = \frac{\dot{m}_m * LHV(m)}{\dot{m}_m * LHV(m) + \dot{m}_d * LHV(d)}$$

where $\dot{m}_m$ and $\dot{m}_d$ represent the mass flow rate of methanol and diesel consumed, and LHV(m) and LHV(d) represent the lower heating values of methanol and diesel, respectively. This study evaluated three premixed methanol ratios: M30, M50, and M80 corresponding to 30, 50, and 80% diesel energy displacement by methanol, respectively. The deviations in obtaining these specific premixed ratios in dual-fuel operation were ±2%. The performance and emission characteristics of the DFC mode using optimised ECU were compared with baseline diesel mode using stock ECU. Various fuel properties of methanol and diesel are given in Table 2.

All measurements for baseline diesel were taken in OEM configuration, without any hardware or software modifications. For methanol-diesel DFC experiments, OEM ECU was replaced by the open ECU for analysing the effect of diesel injection parameters (diesel injection timings and FIP) on the test engine performance and emission characteristics. The OEM wiring harness was also replaced. All essential sensors were calibrated, and the calibration data was included in the open ECU software (M1 Tune). Fuel injection timing and pressure sweeps were carried out for all Genset loads. The diesel injection timing was optimised with constraints of engine knocking, brake-specific energy consumption (BSEC), and visible white smoke (representing unburnt hydrocarbons). The FIP was also kept to the lowest value to avoid wall impingement of the diesel spray. It is more likely to happen in lower ambient temperatures in higher MPR conditions. Methanol was injected in the inlet manifold during intake at 4 bar FIP. The injection quantity was varied by controlling the injector's pulse width, controlled by a micro-controller-based injector driver module.

Initially, the experiments were conducted to study the effect of different premixed ratios of methanol on the performance

Table 1
Technical specifications of the test engine.

Engine Parameters	Specifications
Make/Model	FG-Wilson Diesel Generator/FBD2-1.2D2
Engine type	Four-stroke, two-cylinder, constant-speed, common-rail direct-injection (CRDI) turbocharged CI engine
Fuel Injection System	CRDI/HSD, Delphi, Dual fuel filter system
Aspiration	Turbocharged-Intercooled (TC-IC)
Turbocharged Pressure	1.5 ± 0.3 bar (absolute)
Rated Power	16.2 kW
Rated Engine Speed	1500 rpm
Bore/Stroke	87 mm/100 mm
Displacement Volume	1.2 L
Compression Ratio	17.5
Governor Type	Electronic/Isochronous
Cooling System/Capacity	Liquid Cooled/5.5 L
Lubricating System	Oil Sump, Engine mounted lube oil pump & cooler, Full flow spin-on lubricating oil filter
Lubricating Oil Type	15W40
Lubricating Oil Capacity	4.5 L

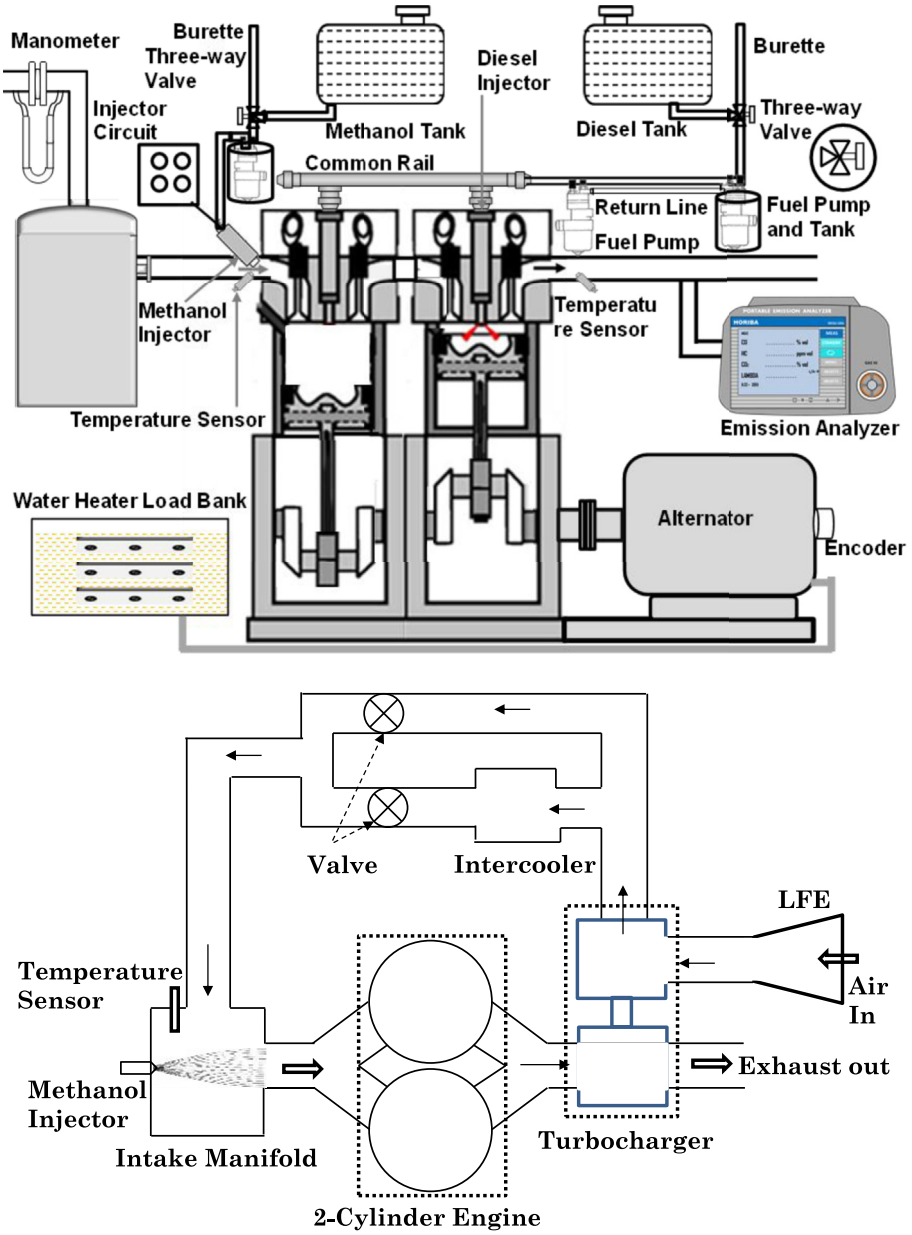

Fig. 1. Schematic of the experimental setup showing the positioning of exhaust plenum, turbocharger, laminar flow equipment (LFE), intercooler, temperature sensor, methanol injector, intake manifold.

characteristics of the Genset engine at varying loads. For this, diesel injection timing was maintained fixed at 3° CA bTDC and the FIP was maintained at 500 bar. In addition, the inlet air temperature was maintained at 42 ± 2 °C at all test conditions for methanol-diesel dual-fuel combustion. The location of the temperature sensor was upstream of the methanol injector. Next, only methanol and diesel injection quantities were varied to obtain desired premixed ratio at a specific engine load. Following this, diesel injection parameters were varied to optimumise fuel injection parameters to improve the engine performance and emission characteristics. This included experiments at varying the diesel injection timings (3° CA bTDC, 6° CA bTDC, and 9° CA bTDC) and the FIP of diesel (500 bar, 750 bar, and 1000 bar).

3. Results and discussion

The results and discussion section is divided into five sub-sections. In the first sub-section, the effect of variations in MPR on the engine performance characteristics (Brake thermal efficiency (BTE), brake specific energy consumption (BSEC), and exhaust gas temperature (EGT)) is compared with conventional diesel combustion (CDC) at varying loads. The impact of MPR and diesel injection timings on emissions (HC, CO, CO_2, NOx, and Smoke Opacity) was investigated at varying engine loads in the second sub-section. The injection timing was in the range of 3°–9° CA bTDC to avoid the engine knocking and NOx formation. The effect of different diesel FIP on emissions was investigated for M50 in the

Table 2
Important properties of diesel and methanol [12,28–30].

Fuel Properties	Diesel	Methanol
Calorific Value (MJ/kg)	44.26	19.76
Kinematic Viscosity (mm^2/s) @ 40 °C	2.96	0.798
Density (g/cm^3) @ 30 °C	0.837	0.783
Carbon Content (%)	86	38
Hydrogen Content (%)	13	12
Oxygen Content (%)	–	50
Autoignition Temperature (°C)	250	450
Latent Heat of Vaporisation (kJ/kg)	250	1110
Cetane Number	54.7	12
Stoichiometric Air-Fuel Ratio	14.4	6.47
Higher Flammability Limits vol%	0.6–7.5	6.7–36
Boiling point (°C)	188–343	65
Burning Velocity (cm/s) (@ 197 °C & 1 atm pressure)	86.7	83.5
Adiabatic flame temperature (°C)	2286	1870
Minimum Ignition energy (mJ)	20	0.14

third sub-section. Finally, correlations between the Smoke Opacity-NOx variations and the NOx-efficiency variations were compared at optimised diesel injection parameters in the fourth and the fifth sub-sections.

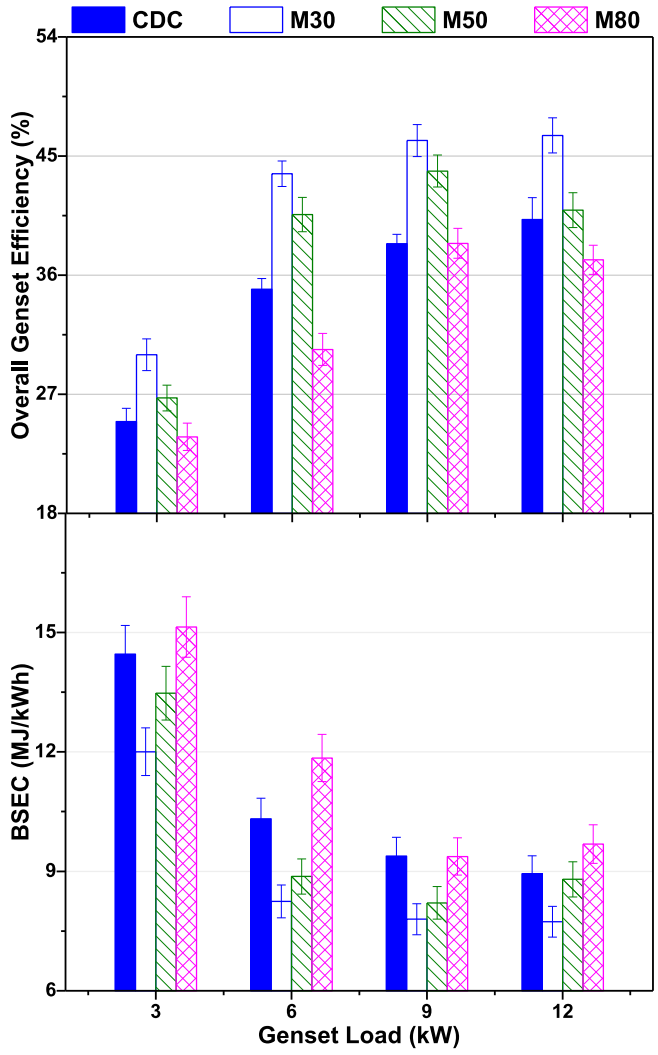

Fig. 2. Effect of MPR on overall BTE (top) and BSEC (bottom) of the engine at varying loads.

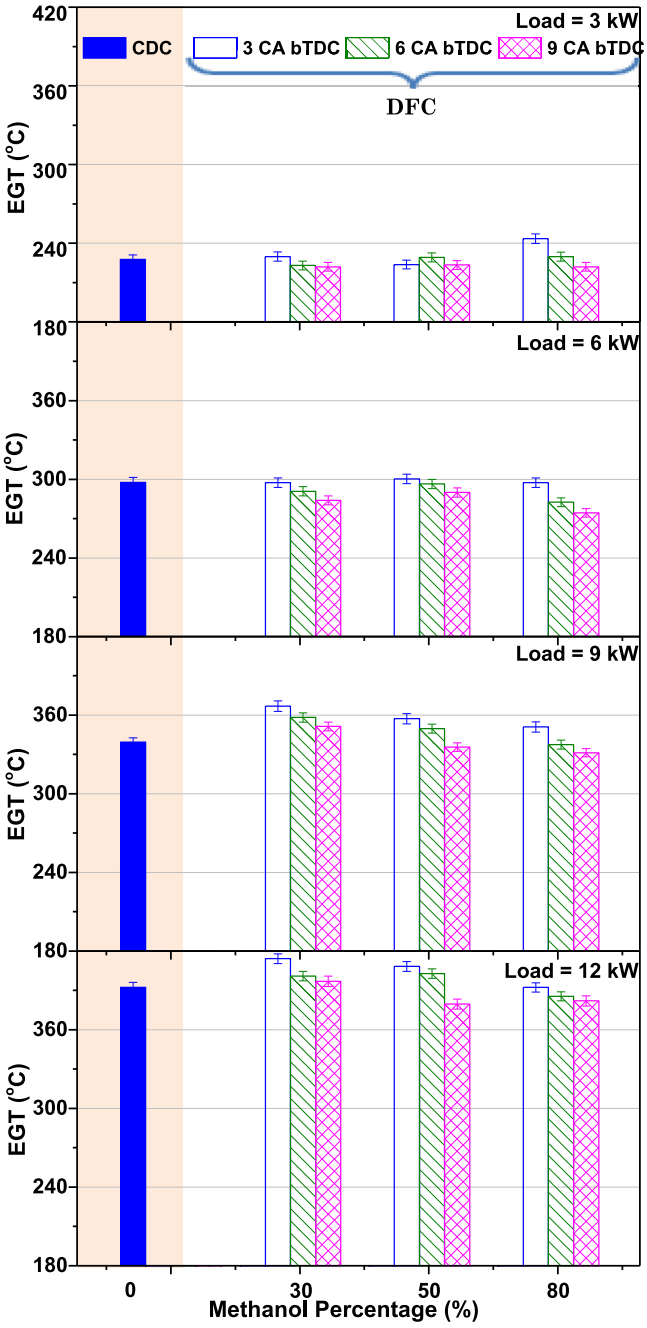

Fig. 3. EGT variations with methanol percentages and fuel injection timings of mineral diesel at different Genset loads in methanol-diesel DFC strategy.

3.1. Effect of MPR on the engine performance characteristics

Figs. 2 and 3 show the performance characteristics of the test engine fuelled with different premixed ratios of methanol in the methanol-diesel DFC mode. The methanol injection quantity was varied simultaneously with diesel to obtain different MPR (30%, 50%, and 80%) while keeping other parameters constant.

The Genset engine was operated with stock ECU with OEM maps to generate baseline data for the CDC mode. For methanol-diesel DFC mode operation, diesel injection timing was kept fixed at 3° CA bTDC and the FIP was maintained at 500 bar. Methanol was injected at 4 bar FIP in the inlet port. Fig. 2 (overall Genset

efficiency) showed that methanol's premixing affected the engine's efficiency differently, depending on the premixed ratio and mixture homogeneity. With an increasing load, overall Genset efficiency increased for all test fuels. At higher engine load, combustion temperature increased due to combustion of higher fuel mass; hence the degree of incomplete combustion and amount of unburnt/partially oxidised hydrocarbons reduced. Hence the Genset efficiency increased for all test fuels with increasing Genset load due to improved combustion efficiency. M30 augmented the Genset efficiency by the highest amount w.r.t. baseline diesel at all loads in the DFC mode.

Furthermore, a higher gain in efficiency was achieved at a higher Genset load. Premixing a lower amount of methanol enhanced the Genset efficiency mainly due to methanol's properties and the premixed charge (methanol) present in the combustion chamber just before the diesel injection. Ignition of diesel spray leads to initiation of combustion of the lean homogeneous methanol-air charge. Rapid heat release by methanol premixed combustion might be delayed after a few crank angle degrees due to the delayed chemical kinetics of pre-combustion reactions. Diesel's diffusion-controlled combustion mainly dominated this enhanced overall heat release, hence benefitted in pushing the piston with greater thrust. This could be a probable reason for higher work output and efficiency. Oxygen enriched charge due to methanol also improved the combustion efficiency.

Similar findings of delayed combustion due to higher ignition delay of methanol because of premixing were also reported [17,31]. In a study by Wang et al. [32], the major reasons for higher BTE of diesel-methanol DFC mode were reduced compression work due to methanol induction and reduced exhaust energy losses due to shorter combustion duration. The hydroxyl group in methanol might have resulted in higher OH radicals in the combustion zone, increasing the oxidation rate of combustion products, which accelerated the combustion [33]. In addition, decreasing the diesel energy share could have reduced the heat losses due to lower flame impingement on the walls. Shorter combustion duration and relatively lower combustion temperature also create favourable conditions for reducing the heat losses. The engine efficiency was slightly higher for M50 than CDC at 3 kW Genset load and improved with increasing the load. Combustion deteriorated for a higher premixed ratio of methanol at a lower Genset load, mainly because the combustion temperature was already low at lower loads, further reduced with induction of large methanol quantity, which has relatively higher heat capacity. Hence, these conditions are not conducive for sustaining the combustion effectively, leading to lower Genset efficiency. However, at higher loads, higher combustion temperatures were experienced. For M50, overall combustion energy was equally contributed by the premixed combustion of methanol and diffusion-controlled diesel combustion. Their combined resultant heat release enhanced the power output of the engine. Although, the increase in the efficiency was slightly lower than M30. In the case of M80, the efficiency of Genset deteriorated at all engine loads in comparison to baseline diesel operation, and this deterioration was observed to be lower at higher Genset loads. In M80, most combustion generated heat was contributed by the premixed combustion of methanol. The lower share of energy contributed by diesel's mixing-controlled combustion phase hampered the ignitability of methanol-air mixture; hence net combustion energy released was not enough to generate rated power output [34].

Moreover, higher ignition delay of diesel in ambient having higher methanol fraction delayed the combustion phasing, which reduced the net effective work transfer from the combusting gases to the piston. In addition, because of a large quantity of methanol injection in the inlet manifold, there were greater chances of larger fuel droplets in the combustion chamber in addition to having liquid methanol film formation on the combustion chamber surfaces. Their incomplete combustion resulted in fuel wastage and higher HC emissions, reducing overall Genset efficiency.

From the trends of BSEC shown in Fig. 2, it can be observed that the test cases resulting in higher Genset efficiency exhibit lower BSEC, which is apparent. Hence, the lowest BSEC values were observed for Genset fuelled with M30 in this study.

As shown in Fig. 3, the EGT values obtained for the methanol-diesel DFC strategy were comparable to the baseline diesel injection strategy at all Genset load conditions. At higher Genset loads (9 kW and 12 kW), EGT for M30 and M50 having diesel injection timing at 3°CA bTDC was slightly higher than CDC. The augmented heat release due to methanol's premixed combustion in addition to diesel's diffusion-controlled combustion might have resulted in slightly higher EGT in these cases. Further, methanol has a higher latent heat of vaporisation; and methanol premixing increases the heat capacity of the charge. Both these factors lower the overall charge temperature in the cylinder. Hence, heat transfer losses might be lower for dual-fuel cases due to a lower temperature difference between the in-cylinder gases and the cylinder walls. Hence, this might have resulted in higher exhaust gas temperature. On the other hand, at 9 and 12 kW, 80% premixed methanol cases resulted in lower EGT than that of 30% and 50% premixing. A cooler in-cylinder environment due to higher premixing might have increased the ignition delay of diesel. Delayed combustion offered a shorter time for combustible gases for heat transfer losses, leading to higher EGT. However, delayed combustion results in lower peak cylinder pressure due to higher cylinder volume, leading to lower EGT. Therefore, the dominance scale of these factors affects the EGT. For this case, lower combustible charge pressure might be a major reason for lower EGT for M80 at higher loads. Further, EGT decreased slightly upon advancing the diesel injection timings. Early diesel injection provided more time for heat transfer during the combustion; hence, EGT reduced in the manifold.

3.2. Effect of MPR and diesel injection timings on the emission characteristics

The effect of MPR and diesel injection timings on HC, CO, CO_2, NOx emissions, and smoke opacity is investigated in this subsection. Fig. 4 shows the HC emissions for different engine operating conditions. The HC emissions form because of incomplete oxidation of hydrocarbon fuels. Primary formation of HC takes place in fuel-lean regions, fuel-rich regions, and regions of low temperature. It has been observed that $0.5 < \varphi < 1$ and temperature below 1200 K result in unfavourable ambient conditions for oxidation of hydrocarbons [35].

From Fig. 4, it can be seen that the HC emissions are insignificant for CDC. For methanol-diesel DFC mode, the HC emissions were significant, and they increased with increasing MPR but reduced with increasing Genset load. HC emissions decreased significantly when the Genset load was increased from 3 kW to 6 kW. This was attributed to reduced localised lean charge pockets due to higher fuel mass inducted and higher ambient temperature. Unlike CDC, methanol was premixed and homogenously distributed in the combustion chamber in DFC, and the pilot diesel initiated the ignition of the methanol-air mixture. A significant fraction remained in the piston bowl for diesel direct injections close to the TDC (adopted in this study) [36]. Premixed methanol-air charge in the squish and crevices regions is unlikely to be burned by the diesel flames and consequent premixed combustion of methanol-air mixture in the combustion chamber. This is the main reason for higher HC emissions with higher MPR.

At higher MPR, the ignition delay of the pilot diesel was higher

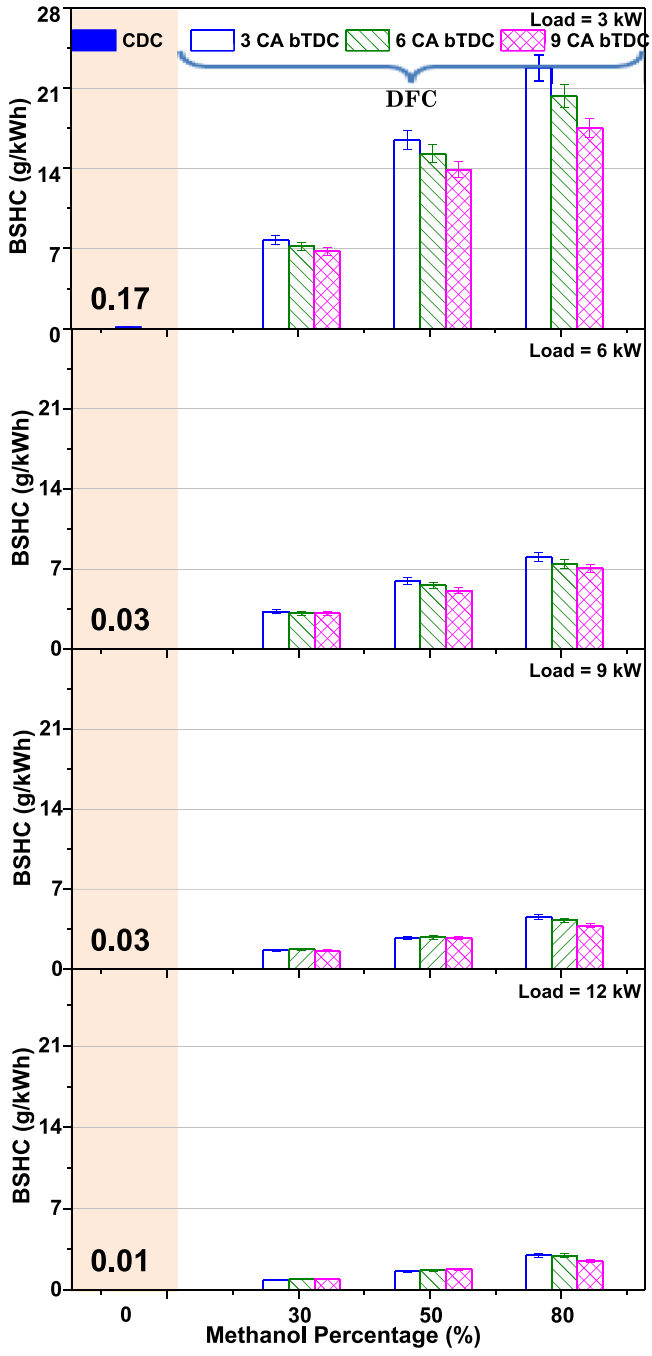

Fig. 4. Brake-specific HC emission variations with methanol percentages and fuel injection timings of mineral diesel at different Genset loads in methanol-diesel DFC strategy.

due to the higher rate of methanol entrainment in the diesel jet. Xu et al. [37] demonstrated that the presence of methanol in the entrained air could decrease the OH radical concentration, inhibiting high-temperature reactions of diesel. A higher ignition delay at higher MPR resulted in a relatively higher energy release in the expansion stroke, delaying combustion and maximum heat release. A similar effect of the low reactivity fuels was reported in several other studies [38,39].

The expansion cooling may further reduce the ambient temperature resulting in decay in the oxidation rate of HC emissions formed [12]. A higher MPR also reduced the peak temperature during compression stroke due to increased specific heat of the charge. The combined effect of these factors was the reason for the observed trends. The HC emissions decreased with advancing diesel injection timings. The most advanced diesel injection timing investigated was 9° CA bTDC, which was relatively closer to the TDC than the injection in usual LTC strategies using premixed combustion. Closer to TDC, the linear velocity of the piston is negligible. Hence it is unlikely that the injected diesel would wet the cylinder walls and enter the crevices, which are important sources of HC emissions. This could probably explain the trends observed in this study. On the other hand, advanced injection timings provide greater residence time to the pilot diesel before the TDC. Therefore, the SoC advances, resulting in a higher fraction of heat release closer to the TDC.

EGT trends also confirmed this justification, as discussed in the previous sub-section. Advanced SoC also resulted in a reduction in expansion cooling. Therefore, the ambient temperature increased, resulting in better oxidation of HC formed in the combustion chamber. The effect of ignition timing seemed more significant at higher MPR and lower Genset loads. For constant Genset load, injected diesel mass decreased with increasing MPR. For the same MPR, injected diesel mass increased with increasing Genset load. Higher diesel mass injected at advanced injection timings results in diesel droplets entering the squish zones, increasing the HC emissions. This counter-effect may be a reason for the relatively lower impact of injection timings at lower MPR and higher Genset loads. A slight increase in the HC emissions was observed for 12 kW load and 50% MPR with advancing diesel injection timings. The increased mass of pilot diesel increased the mixture reactivity in the piston bowl. Thus, the combustion rate increased, resulting in higher in-cylinder temperatures. This was also evident from the increasing EGT trend with increasing Genset load.

The CO emission trends for the study are shown in Fig. 5. The CO emission trends were quite similar to HC emissions. This was attributed to similar fundamental reasons responsible for the formation of both these pollutants. Higher CO emission was observed in CDC mode at the lowest Genset load. CO emission decreased rapidly with increasing in-cylinder temperature. However, with a further increase in the Genset load, CO emission decreased at a relatively lower rate. Lower Genset loads, leaner charge pockets, and low ambient temperatures were the reasons for higher CO emission. With increasing Genset load, the temperature increased. However, higher fuel injection mass at higher Genset load also increased the fuel-rich mixture zones, counter-balancing the effect of temperature. Like HC emission trends, at 12 kW with 50% MPR, CO emission increased with the advancement in diesel injection timing. This further reinforces the argument given earlier. Due to the homogenous nature of methanol distribution in the charge, a significant fuel fraction remains close to the cylinder head. For retarded combustion, the charge in this region flows into the squish region and remains unburned during the cycle. As a result, the ignition is initiated in the piston bowl near the periphery [40]. Therefore, for retarded combustion, the downward motion of the piston further assists this phenomenon.

CO_2 is a desirable combustion product in the engine exhaust since it is the least harmful engine emission. It is produced from the complete combustion of the hydrocarbon fuel in the combustion chamber of an engine. It is a greenhouse gas, though, and lower brake-specific CO_2 emission is desirable.

Fig. 6 shows brake-specific CO_2 emission variation with methanol percentages and diesel injection timing for DFC at different Genset loads at constant engine speed along with CDC. CO_2 emission at a fixed Genset load was nearly constant, and DFC showed lower CO_2 emission than CDC at all Genset loads. Higher efficiency and lower specific energy consumption for M30 could be the reason

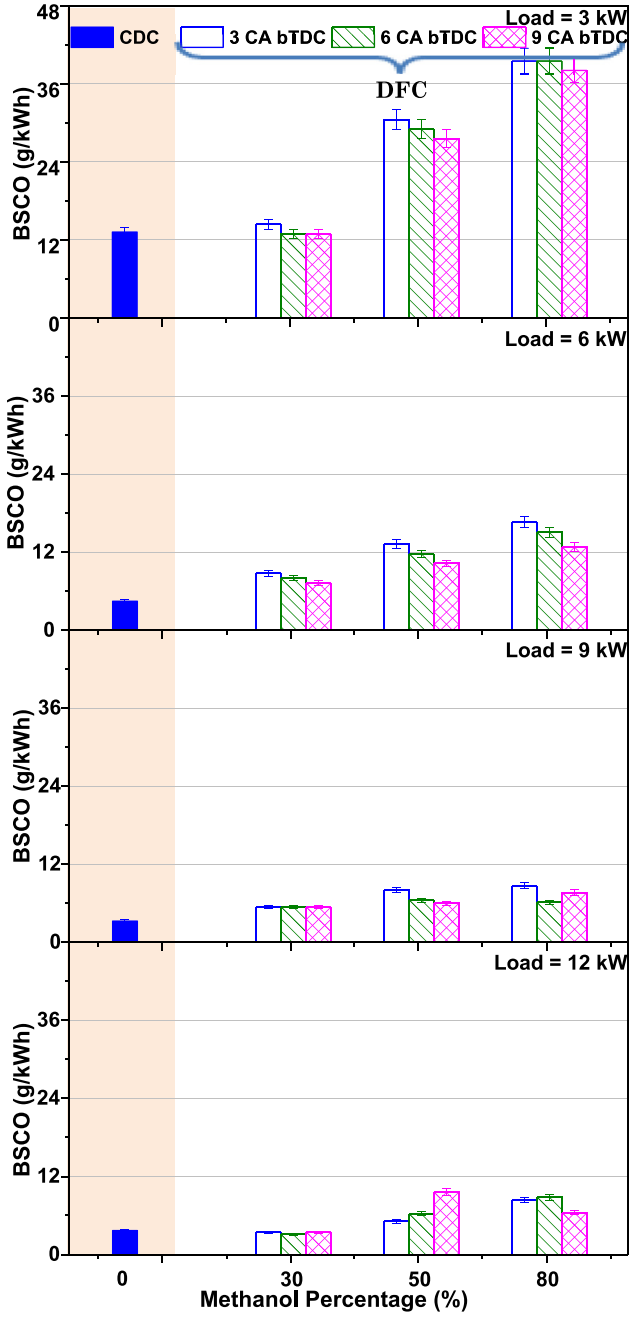

Fig. 5. Brake-specific CO emission variations with methanol percentages and fuel injection timings of mineral diesel at different Genset loads in methanol-diesel DFC strategy.

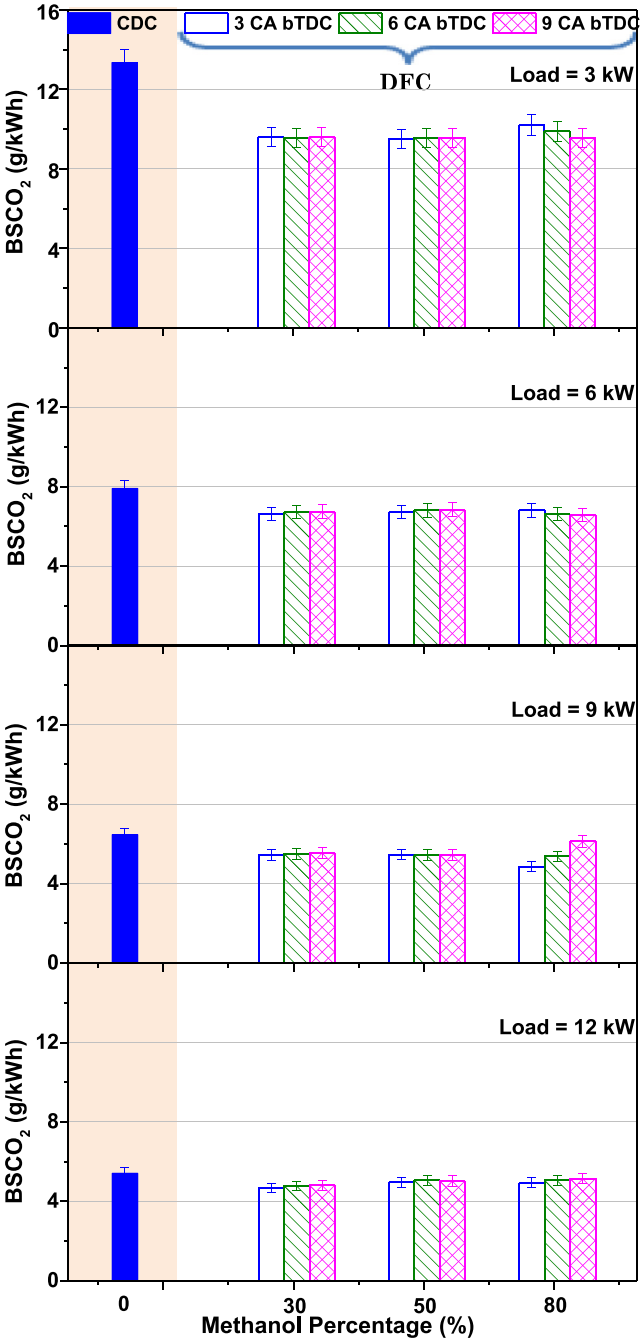

Fig. 6. Brake-specific CO_2 emission variations with methanol percentages and fuel injection timings of mineral diesel at different Genset loads in methanol-diesel DFC strategy.

behind lower CO_2 emissions than CDC. Further, in the high MPR case, despite higher BSEC, methanol's low carbon content decreased the CO_2 emission from the DFC mode operation. As the diesel injection timing advanced, CO_2 emission slightly increased at higher engine loads. However, CO_2 emission variations with increasing methanol percentages were negligible at all engine loads.

NO, and NO_2 are the major constituents of NOx. NO is the main component of NOx in case of complete combustion [41]. The main advantage of methanol application in CI engines is the ultra-low emissions of NOx [18,42]. The NOx emissions are very sensitive to the in-cylinder temperature, and its formation increased rapidly at a temperature greater than 1527 °C [41–45]. NOx is formed due to the oxidation of nitrogen present in the atmosphere at very high in-cylinder temperatures during combustion. NOx formation is mainly governed by the high in-cylinder temperature, excess oxygen availability, and time at extreme conditions [41,45].

Fig. 7 shows the NOx emissions from the Genset engine at different diesel injection timings and MPR for DFC mode w.r.t. baseline CDC mode at varying engine loads. NOx emissions increased as the diesel injection timing was advanced for all test conditions. At retarded diesel injection timing, lower NOx emissions in the DFC mode were observed because of the heat release

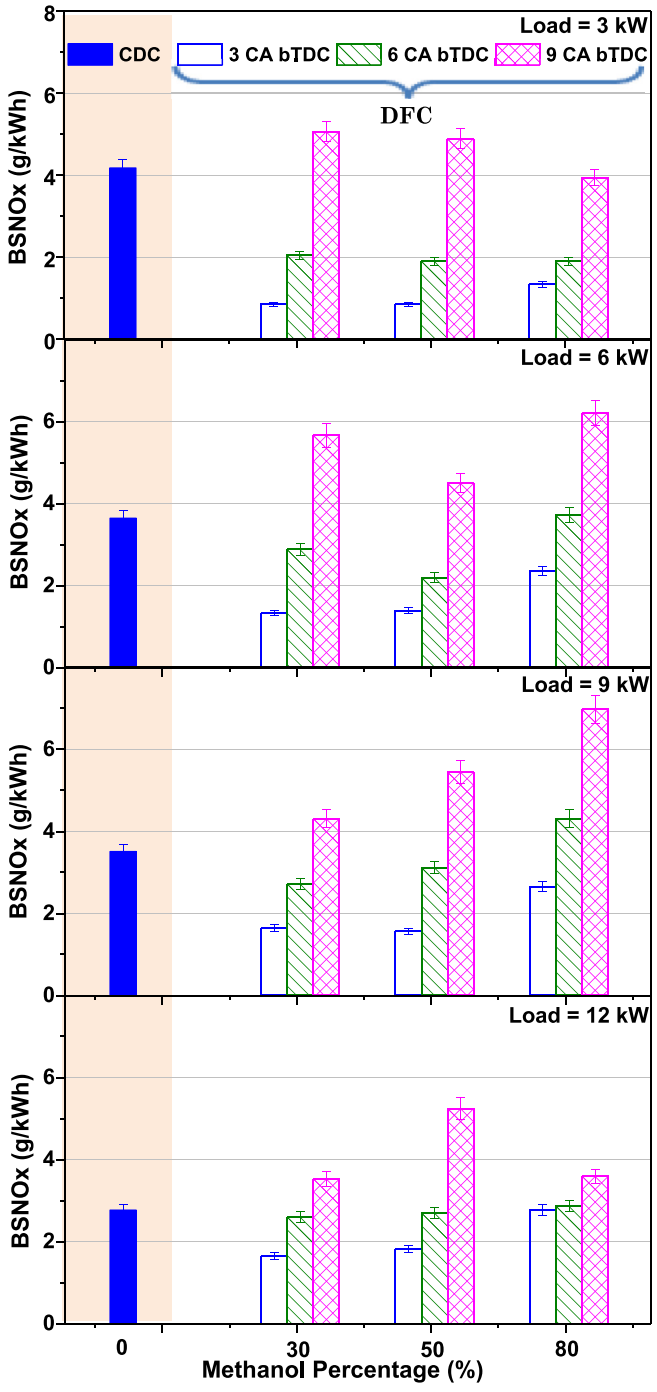

Fig. 7. Brake-specific NOx emissions variations with methanol percentages and fuel injection timings of mineral diesel at different Genset loads in methanol-diesel DFC strategy.

later in the power stroke. The peak in-cylinder temperature of the localised zones was reduced due to expansion cooling. In addition, higher latent heat of vaporisation and heat capacity of methanol-air premixed charge reduced the peak in-cylinder temperature, leading to lower NOx formation [46,47]. The NOx emission reduction was observed especially at the DFC of the lean charge [48]. As diesel injection was advanced, the advanced combustion phasing resulted in a higher heat release rate (HRR). The near TDC heat release increased the peak cylinder temperature and pressure resulting in higher NOx emission. NOx generation is dependent on the reaction time (combustion duration) also [49]. Similar results were also reported by Liu et al. [50].

Brake-specific NOx emissions increased with increasing Genset load at all MPR. After attaining a maximum value at 9 kW Genset load, brake-specific NOx emissions decreased for 6° and 9° CA bTDC. Though, raw emissions of NOx (in PPM) increased with increasing Genset load and advancing diesel injection timings. BTE trends also influenced the NOx emissions, as evident from the NOx trends seen in the CDC mode. Higher NOx emissions at higher Genset load were due to reduced ignition delay, causing combustion of larger fuel quantity in the premixed phase, resulting in higher peak in-cylinder temperature, which promoted the NOx formation [51]. Generally, NOx emissions increased with increasing methanol percentages at 3°, and 6° CA bTDC at all Genset loads, but no definite trend at 9° CA bTDC. For 9° CA bTDC, NOx emissions at 3 kW Genset load decreased with an increasing MPR, while at 9 kW Genset load, they were in the increasing order. At 6 kW Genset load, NOx emissions decreased up to 50% MPR and then increased with 80% MPR at 9° CA bTDC diesel injection timing. The trend, however, reversed at 12 kW Genset load. Increased NOx emissions with increasing MPR may be due to the oxygen content in methanol, increasing oxygen availability in the high-temperature combustion zone and increasing the NOx formation. The other reason may be lower in-cylinder temperature because of the premixing of methanol, leading to greater heat release in the premixed phase and higher temperature yielding higher NOx [52]. An important observation from this graph is that the NOx emissions in methanol-diesel DFC mode are relatively lower than the CDC mode at retarded diesel injection timings. However, NOx emissions increased with advancing diesel injection timings. The lowest reduction in NOx emissions was observed for 3° CA bTDC and 30% MPR at 3 kW Genset load.

The smoke opacity is measured by reducing the light passing through a tube filled with the exhaust gas. Smoke opacity is a qualitative measure of particulate matter emitted by the engine in the exhaust. Smoke opacity is correclated with the larger particulates present in the exhaust gas.

Fig. 8 shows the variations of smoke opacity with MPR in DFC mode at different injection timings of diesel and CDC at different Genset loads. In general, smoke opacity increased with advancing diesel injection timing for DFC at all Genset loads. The CDC showed slightly lower smoke opacity at lower load (3 kW) than DFC mode, while this trend was the opposite at higher Genset loads (9 kW and 12 kW). Higher HC emissions in DFC mode operation at lower Genset loads might be possible for the higher smoke opacity. However, at higher loads, non-sooty exhaust due to oxygen in methanol might have resulted in better combustion in the fuel-rich zone than mineral diesel-fuelled CDC [51]. The smoke opacity variations with MPR were different at varying Genset loads. However, CDC mode exhibited lower smoke opacity than the DFC mode at 3 kW Genset load. For 6 kW Genset load, Smoke opacity for 3° and 6° CA bTDC diesel injection timing were nearly identical, and both decreased with an increasing MPR. However, at 9° CA bTDC diesel injection timing, smoke opacity increased from 30% to 50% MPR before decreasing at 80% MPR. At 9 kW Genset load, smoke opacity decreased with increasing MPR at all diesel injection timings. Smoke opacity was the maximum for CDC and the lowest for 3° CA bTDC diesel injection timing at 80% MPR. The smoke opacity at 12 kW Genset load was different for all MPR in DFC mode, and its variation was random. Smoke opacity at 12 kW load first increased with increasing MPR and then decreased in DFC mode. However, the CDC mode exhibited a much higher value than other loads and diesel injection timings in DFC mode. The smoke opacity was the maximum for the CDC mode at 12 kW Genset load. In general, with diesel injection timing advance in DFC mode, smoke opacity

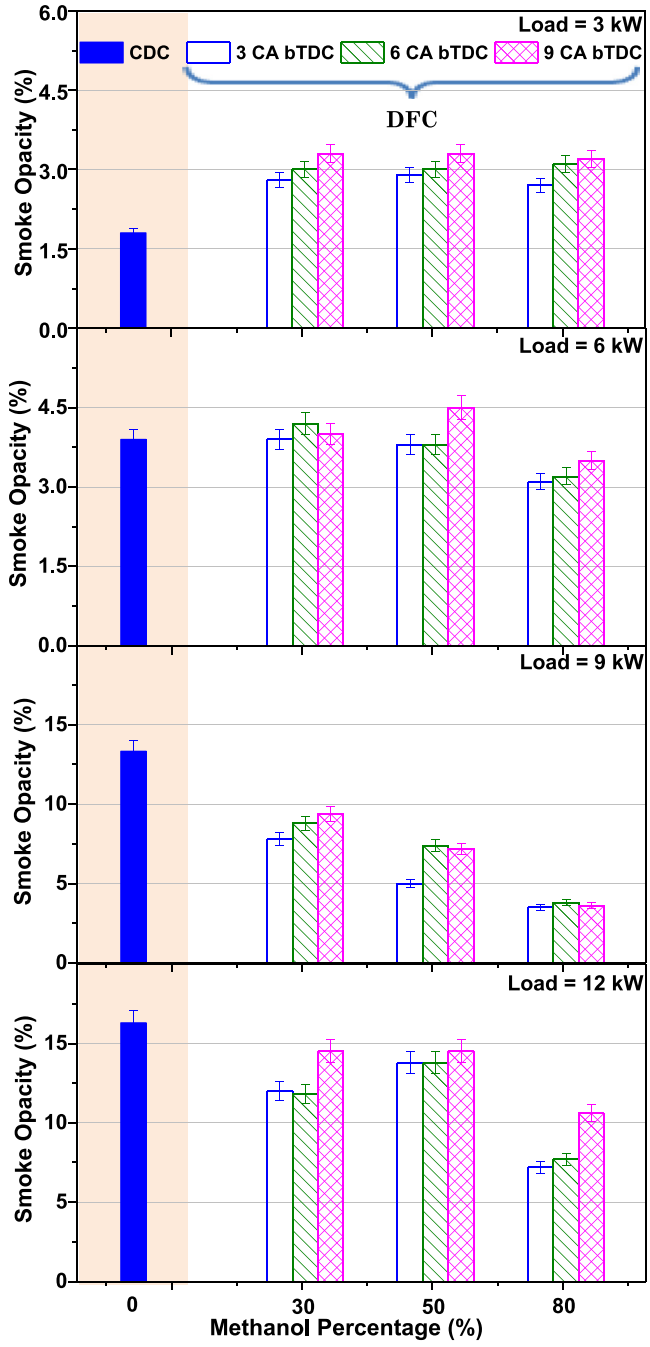

Fig. 8. Smoke opacity variations with methanol percentages and fuel injection timings of mineral diesel at different Genset loads in methanol-diesel DFC strategy.

increased at all MPR. The overall trend of smoke opacity is that exhaust soot emission in CDC mode of Genset engine is higher at higher load. It decreased with methanol induction in the inlet port in DFC mode.

The study's main objective was to replace the maximum amount of diesel with methanol without compromising the engine performance and emissions. After comparing the different MPRs in dual-fuel operation, it was found that M50 was suitable from both performance and emissions points of view. M50 exhibited higher BTE, along with the reductions in NOx and smoke emissions. Hence, M50 was selected for further diesel injection parameter optimisation. With further tests, 3° bTDC diesel injection timing was found suitable at all engine loads, considering all emissions. Advancing injection timing resulted in significantly higher NOx emissions. Hence, M50 with 3° bTDC diesel injection was chosen for investigating the effect of diesel injection pressure.

3.3. Effect of diesel injection pressure on regulated emissions

After investigating the effects of diesel injection timings on engine performance and emissions in the DFC mode engine in the previous sub-sections, diesel FIP was varied (500, 750, and 1000 bar) to investigate its effect on the engine-out emissions. The emission tests were conducted for M50 while keeping the diesel injection timing fixed at 3° CA bTDC, while the diesel FIP was varied. The emissions from DFC mode at varying diesel injection timings were compared with the CDC mode at different Genset loads.

Fig. 9 shows the brake-specific emissions and smoke opacity variations with Genset load at three Diesel FIP at fixed injection timings in DFC mode with 50% MPR compared to baseline CDC mode.

The BSCO emission first increased and then decreased slightly with the FIP increase at a lower load (3 kW). However, increasing diesel FIP at all Genset loads decreased the brake-specific HC emissions. This was due to improved spray atomisation of diesel and better mixing with the premixed charge present in the combustion chamber, leading to better combustion. The improved combustion leads to oxidation of HC to CO, increasing CO emission [53,54]. With further increase in the FIP, the in-cylinder temperature increased, assisting the oxidation of CO further. The increased temperature is evident from the NOx emission trend, which increased with the FIP. The trend of CO emission with the FIP was similar at higher engine loads. Both HC and CO emissions decreased due to improved oxidation because of increased engine load, leading to higher in-cylinder temperature.

On the other hand, Brake-specific NOx emissions increased with increasing diesel FIP. This is also because of better combustion, resulting in relatively higher in-cylinder temperature, leading to more NOx formation. The DFC mode emitted lower NOx than the CDC mode, except at 1000 bar diesel FIP. Smoke opacity decreased with increasing diesel FIP in the DFC mode, except for 9 kW Genset load. At 9 kW Genset load, smoke opacity first increased and then decreased with increasing diesel FIP. At lower Genset loads, smoke opacity in DFC mode at all FIP was higher than in the CDC mode. However, the CDC mode exhibited higher smoke opacity at higher loads than the DFC mode at all diesel FIPs. At low loads, higher smoke in dual-fuel mode than CDC might be due to deteriorated combustion, as also observed from higher HC and CO emissions. Due to 50% premixing in low load conditions, methanol evaporative cooling might have lowered the combustion temperature. This incomplete combustion was seen as higher smoke emissions. However, higher combustion temperature at high loads resulted in improved combustion of premixed methanol. Also, in CDC, the combustion was mainly diffusion-controlled, resulting in higher particulate emissions than partially premixed combustion phase in the dual-fuel mode. The main outcome of this study is that HC emissions and smoke opacity can be reduced by increasing the diesel FIP in DFC mode. Diesel FIP of 750 bar in DFC mode resulted in a good trade-off between HC and NOx emissions. A higher diesel FIP significantly reduced the HC emissions at a low load.

3.4. Effect of MPR on smoke Opacity-NOx trade-off

The trend of smoke opacity qualitatively reflects the trend for soot emissions from the engine. Fig. 10 shows the correlation between the NOx emissions and smoke opacity variations with the

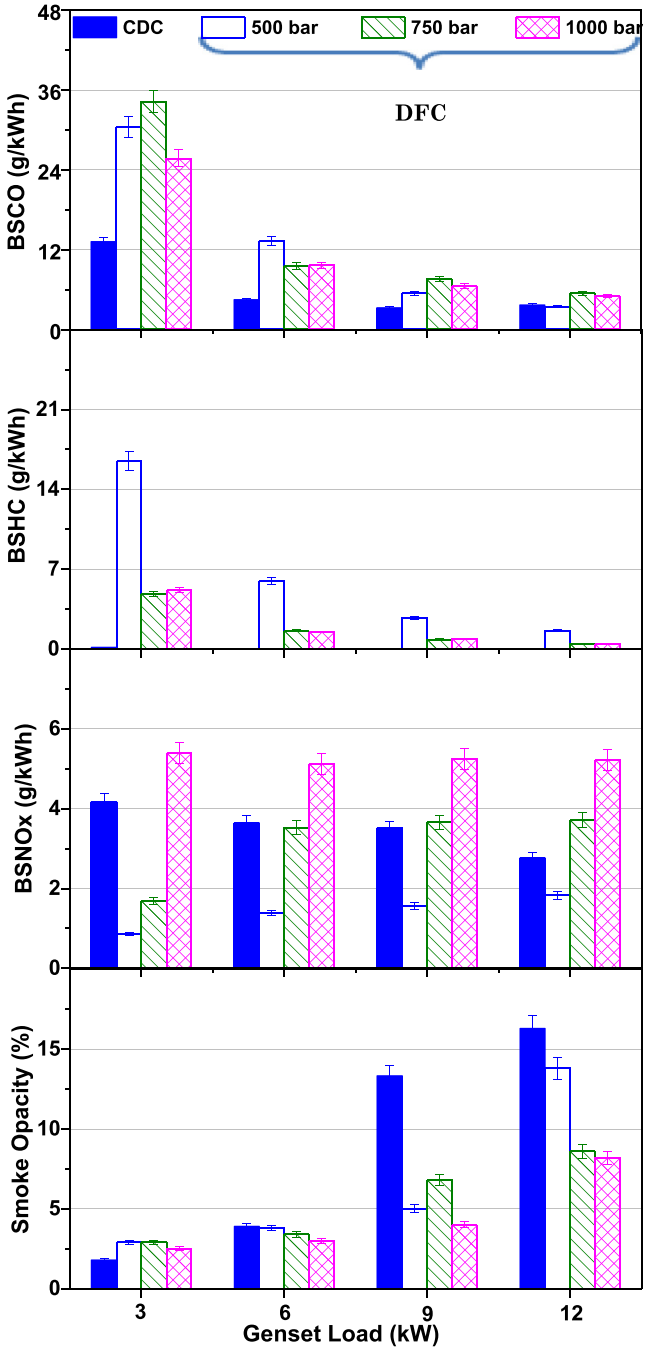

Fig. 9. Emissions in DFC mode at varying diesel FIP w.r.t. Genset load for 50% MPR.

MPR. The experimental data are presented for 6 and 9 kW Genset loads, diesel injection timing of 3° CA bTDC and diesel FIP of 500 bar in DFC mode.

The MPR range was divided into three regions based on the NOx and Smoke opacity in the DFC mode. The left-most border data point represents the baseline CDC mode NOx emissions and Smoke opacity. These three regions were high NOx and soot, low NOx and soot, and high NOx-low soot regions. The intersection point of the NOx emissions and smoke opacity in the low NOx and soot region showed a trade-off point of NOx-soot. This qualitative analysis of NOx and smoke opacity exhibited the NOx and soot emissions in the CDC and DFC modes. The vertical or horizontal shifting of the

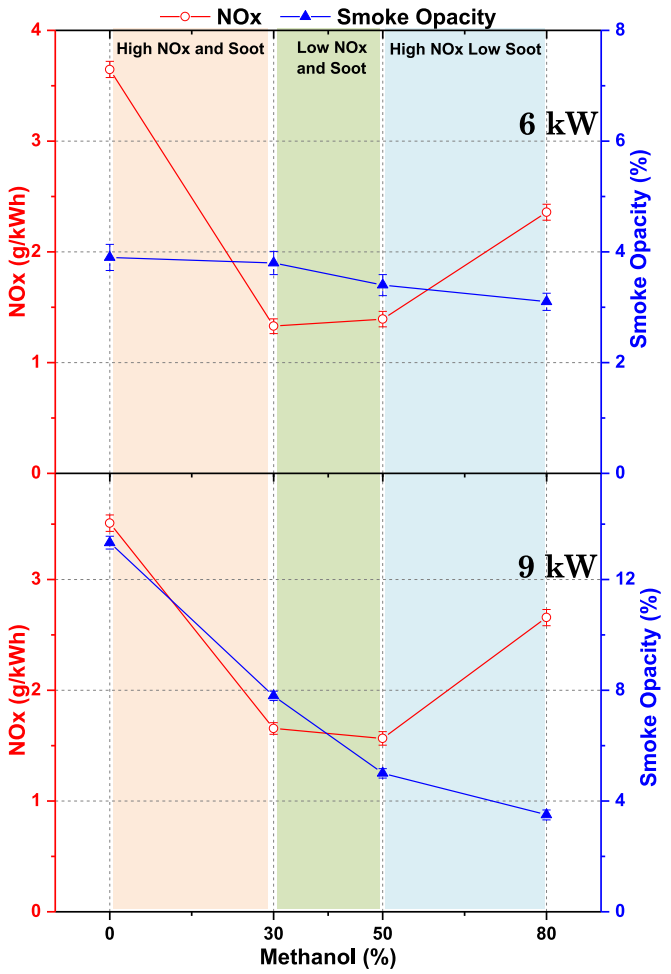

Fig. 10. Correlation between NOx and Smoke Opacity variations with MPR at 9 kW Genset load having 3° CA bTDC diesel injection timing and diesel FIP of 500 bar in DFC mode.

trade-off point showed the combustion effectiveness in suppressing the NOx and soot emissions. A smaller area below the NOx and smoke opacity lines showed better NOx and soot reduction. NOx and soot emissions in CDC mode were higher than in the DFC mode. In DFC mode, as MPR increased, the NOx and soot decreased up to 50% MPR at 9 kW Genset load; however, at 6 kW Genset load, they remained constant. The NOx emissions increased beyond 50% MPR while soot emissions reduced up to 80% MPR. This qualitative analysis of NOx and smoke opacity reflected that NOx and soot emissions were the lowest for MPR between 30% and 50% and lower for 6 kW Genset load than 9 kW.

3.5. *Effect of MPR on correlation between overall genset efficiency and NOx*

Fig. 11 represents the NOx emissions and overall Genset efficiency correlation with the MPR at 6 and 9 kW Genset loads for CDC and DFC modes, at diesel injection timing of 3° CA bTDC and diesel FIP of 500 bar.

This graphical correlation in Fig. 11 is divided into three distinct regions: high NOx and medium efficiency (starting from 0 to 30% MPR), low NOx and high efficiency (ranging from 30% to 50% MPR), and medium NOx and lower efficiency (ranging from 30% to 80% MPR). The central region showed a high Genset efficiency and low NOx emissions. There were two intersection points/saddle points,

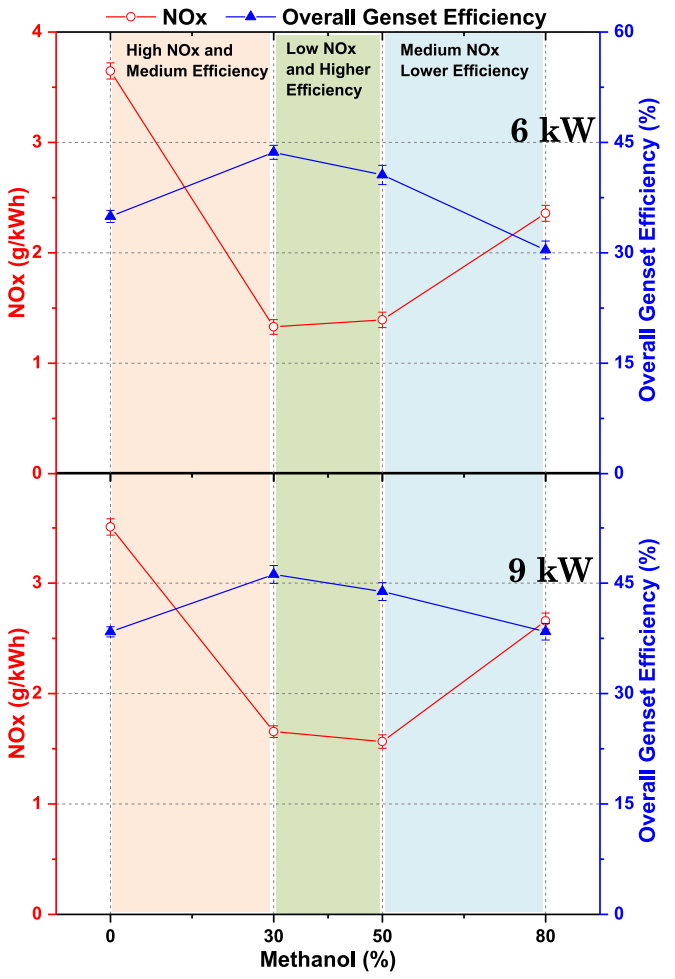

Fig. 11. Correlation between NOx and overall Genset efficiency variations with MPR at 9 kW Genset load having 3° CA bTDC diesel injection timing and diesel FIP of 500 bar in DFC mode.

at which efficiency and NOx emissions change their slope. The left-most saddle point-1 was high NOx medium efficiency, and the right-most saddle point-2 was at medium NOx lower efficiency. Right movement of saddle point-1 and left movement of saddle point-2 showed excellent Genset engine combustion. The area between these two saddle points represents higher overall Genset efficiency and lower NOx emissions. The main reasons for NOx emissions have been identified as high combustion temperature, and availability of excess oxygen, according to the Zeldovich mechanism [42]. However, Fig. 11 shows that increasing methanol fraction from M30 to M50 resulted in reductions in the BTE and NOx emissions at 9 kW engine load. On the other hand, the NOx emissions remained constant at a 6 kW engine load. Further increasing the methanol fraction from M50 to M80 resulted in a reduction in BTE with an increase in NOx emissions at both loads. This might be attributed to suitable combustion phasing, better combustion quality, and lower heat losses for lower methanol premixing, i.e., M30, compared to the CDC mode, which improved the BTE. With increasing methanol ratio to M50 and M80, BTE decreased due to deteriorated combustion and delayed combustion phasing. However, the role of charge cooling due to methanol premixing in reducing the NOx emissions was only observed till M50. For M80, excess oxygen availability due to the large presence of methanol combustion might have altered the trend, resulting in higher NOx emissions. Similar behaviour of BTE and NOx emissions was reversed when changing the proportion of gasoline-diesel RCCI combustion from 50/50 to 75/25 [55]. For a higher premixed quantity of gasoline, a delayed and extended heat release rate was observed. The high temperature during the extended period of heat release resulted in increased NOx emissions. Hence, this might also be a possible reason for higher NOx emissions in this study.

The qualitative correlation between overall Genset efficiency and NOx emissions exhibited maximum efficiency at 30% MPR. The DFC mode engine obtained minimum NOx emissions at 50% MPR. This qualitative study experimentally demonstrated that a DFC mode engine exhibited a superior performance and emissions for a medium range of MPR (30–50%).

4. Conclusions

This experimental study was performed to investigate the performance and emissions characteristics of the diesel-methanol DFC mode engine vis-a-vis conventional diesel combustion (CDC) mode engine operation. The objective was to find optimum parameters for superior engine performance in DFC mode, with significant Methanol utilisation in the engine. The diesel injection timings and MPR were varied in the DFC mode, and their effect on engine performance and emissions was investigated and compared with baseline CDC mode. This study concluded that the overall Genset efficiency increased in DFC mode compared to the baseline CDC mode, except at higher MPR (80%). The maximum overall Genset efficiency increased by 20.3% at 9 kW Genset load and 30% MPR. Higher HC and CO emissions were observed in DFC mode than baseline CDC mode. Brake-specific NOx emissions decreased with increasing MPR but worsened at advanced diesel injection timings. NOx emissions at 3° CA bTDC were always lower in DFC mode than the baseline CDC mode. Smoke opacity was lower in the DFC mode than the CDC mode at higher Genset load. With advancing diesel injection timings and increasing MPR at higher loads, these values decreased. In DFC mode, HC, CO, and smoke opacity reduced upon increasing diesel FIP; however, NOx emissions increased. A FIP of 750 bar and injection timing of 3° CA bTDC were optimum at lower loads. EGR can be explored to tackle the NOx emissions at advanced injection timings and higher FIP in DFC mode. Moderate diesel FIP and retarded diesel injection timing offered the best trade-offs for HC and NOx emissions. Overall, Genset efficiency can be enhanced, and NOx and soot emissions reduced by port injection of methanol (30–50% on an energy basis) and bypassing turbocharged air to maintain inlet charge temperature constant.

Credit author statement

Conceptualization by AKA and VK; Data curation VK, AJ and AK; Formal analysis VK, AJ and AK; Investigation VK, AJ and AK; Methodology AKA; Project administration AKA; Resources AKA; Supervision AKA; Validation VK; Writing – original draft VK, AJ and AK; Writing – review & editing AKA.

Declaration of competing interest

The authors declare the following personal relationships which may be considered as potential competing interests: 1. Prof. Ashwani Gupta. Department of Mechanical Engineering. University of Maryland, USA. 2. Prof. S K Aggarwal. Mechanical Engineering Department. University of Illinois, Chicago, USA.

Acknowledgements

Financial support from the Council for Scientific and Industrial

Research (CSIR) Government of India's SRA scheme to Dr Vikram Kumar is gratefully acknowledged, which supported his stay at ERL, IIT Kanpur for conducting these experiments.

References

[1] Liu Y, Li G, Chen Z, Shen Y, Zhang H, Wang S, Qi J, Zhu Z, Wang Y, Gao J. Comprehensive analysis of environmental impacts and energy consumption of biomass-to-methanol and coal-to-methanol via life cycle assessment. Energy 2020;204:117961.

[2] Valera, H., Agarwal, A.K. Methanol as an alternative fuel for diesel engines. In Methanol and the alternate fuel economy 2019; 9-33. Springer, Singapore.

[3] Schweitzer C. Synthesising strengths of 1st and 3rd generation biorefineries. Biomethanol as a biorefinery product. Int Sugar J 2014:64–70.

[4] Gardiner M. Energy requirements for hydrogen gas compression and liquefaction as related to vehicle storage needs. 2009 [online].

[5] Steinberg M. Synthetic carbonaceous fuels and feedstocks from oxides of carbon and nuclear power. Fuel 1978;57(8):460–8.

[6] Steinberg M. Methanol as an agent for CO_2 mitigation. Energy Convers Manag 1997;38:S423–30.

[7] Pearson RJ, Turner JWG. Renewable fuels: an automotive perspective. In: Comprehensive renewable energy. Elsevier Ltd; 2012. p. 305–42.

[8] Kumar V, Agarwal AK. Friction, wear, and lubrication studies of alcohol-fuelled engines. Advances in engine tribology. Singapore: Springer; 2022. p. 9–29.

[9] Jackson M, Unnasch S, Sullivan C, Renner R. Transit bus operation with methanol fuel. SAE Trans 1985;94:50–61.

[10] Landälv I. Methanol as a renewable fuel—a knowledge synthesis. Fuels: The Swedish Knowledge Centre for Renewable Transportation; 2017. p. 6.

[11] Dong Y, Kaario O, Hassan G, Ranta O, Larmi M, Johansson B. High-pressure direct injection of methanol and pilot diesel: a non-premixed dual-fuel engine concept. Fuel 2020;277:117932.

[12] Verhelst S, Turner JW, Sileghem L, Vancoillie J. Methanol as a fuel for internal combustion engines. Prog Energy Combust Sci 2019;70:43–88.

[13] Li Y, Jia M, Chang Y, Liu Y, Xie M, Wang T, Zhou L. Parametric study and optimisation of a RCCI (reactivity controlled compression ignition) engine fueled with methanol and diesel. Energy 2014;65:319–32.

[14] Dipankar K, Roy S, Banerjee R. Development of an artificial neural network based virtual sensing platform for the simultaneous prediction of emission-performance-stability parameters of a diesel engine operating in dual fuel mode with port injected methanol. Energy Convers Manag 2019;184:488–509.

[15] Ma B, Yao A, Yao C, Wu T, Wang B, Gao J, Chen C. Exergy loss analysis on diesel methanol dual fuel engine under different operating parameters. Appl Energy 2020;261:114483.

[16] Li G, Zhang C, Li Y. Effects of diesel injection parameters on the rapid combustion and emissions of an HD common-rail diesel engine fueled with diesel-methanol dual-fuel. Appl Therm Eng 2016;108:1214–25.

[17] Wei H, Yao C, Pan W, Han G, Dou Z, Wu T, Liu M, Wang B, Gao J, Chen C, Shi J. Experimental investigations of the effects of pilot injection on combustion and gaseous emission characteristics of diesel/methanol dual fuel engine. Fuel 2017;188:427–41.

[18] Park S, Cho J, Park J, Song S. Numerical study of the performance and NOx emission of a diesel-methanol dual-fuel engine using multi-objective Pareto optimisation. Energy 2017;124:272–83.

[19] Panda K, Ramesh A. Diesel injection strategies for reducing emissions and enhancing the performance of a methanol based dual fuel stationary engine. Fuel 2021;289:119809.

[20] Krishnamoorthi M, Sreedhara S, Duvvuri PP. The effect of low reactivity fuels on the dual fuel mode compression ignition engine with exergy and soot analyses. Fuel 2021;290:120031.

[21] Guan W, Wang X, Zhao H, Liu H. Exploring the high load potential of diesel–methanol dual-fuel operation with Miller cycle, exhaust gas recirculation, and intake air cooling on a heavy-duty diesel engine. Int J Engine Res 2021;22(7):2318–36.

[22] Saxena MR, Maurya RK. Effect of premixing ratio, injection timing and compression ratio on nano particle emissions from dual fuel non-road compression ignition engine fueled with gasoline/methanol (port injection) and diesel (direct injection). Fuel 2017;203:894–914.

[23] Dou Z, Yao C, Wei H, Wang B, Liu M, Chen C, Gao J, Shi J. Experimental study of the effect of engine parameters on ultrafine particle in diesel/methanol dual fuel engine. Fuel 2017;192:45–52.

[24] Liu J, Li Y, Li G, Zhu Z, He H, Liu S. Effect of pilot diesel quantity and fuel delivery advance angle on the performance and emission characteristics of a methanol-fueled diesel engine. Energy Fuels 2010;24(3):1611–6.

[25] Reitz RD, Duraisamy G. Review of high efficiency and clean reactivity controlled compression ignition (RCCI) combustion in internal combustion engines. Prog Energy Combust Sci 2015;46:12–71.

[26] Pan W, Yao C, Han G, Wei H, Wang Q. The impact of intake air temperature on performance and exhaust emissions of a diesel methanol dual fuel engine. Fuel 2015;162:101–10.

[27] Sonawane U, Kalwar A, Agarwal AK. Microscopic and macroscopic spray characteristics of gasohols using a port fuel injection system. SAE Technical Paper 2020-01-0324 2020.

[28] Metghalchi M, Keck JC. Burning velocities of mixtures of air with methanol, isooctane, and indolene at high pressure and temperature. Combust Flame 1982;48:191–210.

[29] Kumar V, Singh AP, Agarwal AK. Gaseous emissions (regulated and unregulated) and particulate characteristics of a medium-duty CRDI transportation diesel engine fueled with diesel-alcohol blends. Fuel 2020;278:118269.

[30] Wang B, Yao A, Chen C, Yao C, Wang H, Liu M, Li Z. Strategy of improving fuel consumption and reducing emission at low load in a diesel methanol dual fuel engine. Fuel 2019;254:115660.

[31] Wei L, Yao C, Han G, Pan W. Effects of methanol to diesel ratio and diesel injection timing on combustion, performance and emissions of a methanol port premixed diesel engine. Energy 2016;95:223–32.

[32] Wang B, Yao A, Yao C, Chen C, Wang H. In-depth comparison between pure diesel and diesel methanol dual fuel combustion mode. Appl Energy 2020;278:115664.

[33] Ma B, Yao A, Yao C, Chen C, Qu G, Wang W, Ai Y. Multiple combustion modes existing in the engine operating in diesel methanol dual fuel. Energy 2021;234:121285.

[34] Li G, Zhang C, Li Y. Effects of diesel injection parameters on the rapid combustion and emissions of an HD common-rail diesel engine fueled with diesel-methanol dual-fuel. Appl Therm Eng 2016;108:1214–25.

[35] Kim D, Ekoto I, Colban WF, Miles PC. In-cylinder CO and UHC imaging in a light-duty diesel engine during PPCI low-temperature combustion. SAE International Journal of Fuels and Lubricants 2009;1(1):933–56.

[36] Raman V, Tang Q, An Y, Shi H, Sharma P, Magnotti G, Chang J, Johansson B. Impact of spray-wall interaction on the in-cylinder spatial unburned hydrocarbon distribution of a gasoline partially premixed combustion engine. Combust Flame 2020;215:157–68.

[37] Xu S, Zhong S, Pang KM, Yu S, Jangi M, Bai XS. Effects of ambient methanol on pollutants formation in dual-fuel spray combustion at varying ambient temperatures: a large-eddy simulation. Appl Energy 2020;279:115774.

[38] Kokjohn S, Hanson R, Splitter D, Kaddatz J, Reitz R. Fuel reactivity controlled compression ignition (RCCI) combustion in light-and heavy-duty engines. SAE International Journal of Engines 2011;4(1):360–74.

[39] Singh AP, Sharma N, Kumar V, Agarwal AK. Experimental investigations of mineral diesel/methanol-fueled reactivity controlled compression ignition engine operated at variable engine loads and premixed ratios. Int J Engine Res 2021;22(7):2375–89.

[40] Tang Q, Liu H, Li M, Geng C, Yao M. Multiple optical diagnostics on effect of fuel stratification degree on reactivity controlled compression ignition. Fuel 2017;202:688–98.

[41] Lavoie GA, Heywood JB, Keck JC. Experimental and theoretical study of nitric oxide formation in internal combustion engines. Combust Sci Technol 1970;1:313–26.

[42] Ya B. The oxidation of nitrogen in combustion and explosions. Acta Physicohimica, URRS 1946;21:577–628.

[43] Amnéus P, Mauss F, Kraft M, Vressner A, Johansson B. NOx and N_2O formation in HCCI engines. SAE Technical Paper 2005-01-0126 2005.

[44] Li H, Neill WS, Guo H, Chippior W. The NOx and N_2O emission characteristics of an HCCI engine operated with N-heptane. ICEF 2007-1758, proceedings of ASME internal combustion engine division. South Carolina, USA: Technical Conference ICEF-2007; 2007.

[45] Guo HS, Liu FS, Smallwood G. A numerical study on NOx formation in laminar counter flow CH_4/air triple flame. Combust Flame 2005;143:282–98.

[46] Easley WL, Mellor AM, Plee SL. NO formation and decomposition models for DI diesel engines. SAE Technical Paper 2000-01-0582 2000.

[47] Andersson M, Johansson B, Hultqvist A, Noehre C. A predictive real time NOx model for conventional and partially premixed diesel combustion. SAE Trans 2006:863–72.

[48] Jiang QQ, Ottikkutti P, Vangerpen J, Vanmeter D. The effect of alcohol fumigation on diesel flame temperature and emissions. SAE Technical Paper 900386; 1990.

[49] Yoshikawa T, Reitz RD. Development of an improved NOx reaction mechanism for low temperature diesel combustion modelling. SAE International Journal of Engines 2008;1:1105–17.

[50] Liu J, Yao A, Yaom C. Effects of injection timing on performance and emissions of a HD diesel engine with DMCC. Fuel 2014;134:107–13.

[51] Cheng CH, Cheung CS, Chan TL, Lee SC, Yao CD. Experimental investigation on the performance, gaseous and particulate emissions of a methanol fumigated diesel engine. Sci Total Environ 2008;389:115–24.

[52] Musculus MP, Miles PC, Pickett LM. Conceptual models for partially premixed low-temperature diesel combustion. Prog Energy Combust Sci 2013;39(2–3):246–83.

[53] Jena A, Agarwal AK. Strategical evolution of clean diesel combustion. In: Advanced combustion for sustainable transport, vols. 9–42. Singapore: Springer; 2022.

[54] Imran A, Varman M, Masjuki HH, Kalam MA. Review on alcohol fumigation on diesel engine: a viable alternative dual fuel technology for satisfactory engine performance and reduction of environment concerning emission. Renew Sustain Energy Rev 2013;26:739–51.

[55] Benajes J, Molina S, García A, Belarte E, Vanvolsem M. An investigation on RCCI combustion in a heavy-duty diesel engine using in-cylinder blending of diesel and gasoline fuels. Appl Therm Eng 2014;63(1):66–76.